Genome-wide coorientation of replication and transcription reduces adverse effects on replication in *Bacillus subtilis*

Jue D. Wang*, Melanie B. Berkmen, and Alan D. Grossman†

Department of Biology, Building 68-530, Massachusetts Institute of Technology, Cambridge, MA 02139

Edited by Sue Hengren Wickner, National Institutes of Health, Bethesda, MD, and approved January 29, 2007 (received for review October 11, 2006)

In many bacteria, there is a strong bias for genes to be encoded on the leading strand of DNA, resulting in coorientation of replication and transcription. In *Bacillus subtilis*, transcription of the majority of genes (75%) is cooriented with replication. By using genome-wide profiling of replication with DNA microarrays, we found that this coorientation bias reduces adverse effects of transcription on replication. We found that in wild-type cells, transcription did not appear to affect the rate of replication elongation. However, in mutants with reversed transcription bias for an extended region of the chromosome, replication elongation was slower. This reduced replication rate depended on transcription and was limited to the region in which the directions of replication and transcription are opposed. These results support the hypothesis that the strong bias to coorient transcription and replication is due to selective pressure for processive, efficient, and accurate replication.

DNA microarrays | elongation of replication | genomic organization | genomic stability | origin of replication

Many aspects of the organization of bacterial genomes are conserved and important for cell survival. DNA rearrangements, including large chromosomal inversions, can lead to inviability, decreased fitness, and impaired development (1–4). It has been proposed that genomic organization affects replication, transcription, and segregation of genomes (5).

One benefit of proper genomic organization may be the reduction of potential conflicts between replication and transcription (5–7). The same DNA template is used by RNA polymerase (RNAP) for transcription and by the replisome (DNA polymerase and associated proteins) for replication. Transcription complexes that are stalled, initiating, or terminating can slow or block replication (8, 9). RNAP and the replisome can collide when moving toward each other (head-on), or when the replisome, which moves faster than RNAP, catches up with RNAP moving in the same direction (codirectional). Head-on and codirectional collisions can occur when genes are on the lagging and leading strands, respectively.

The consequences of head-on and codirectional collisions are different. In *Escherichia coli*, high levels of transcription can effectively slow or block progression of replication forks if transcription and replication are head-on, but not if they are codirectional (10). In French's landmark study, an inducible plasmid-derived origin of replication was positioned on either side of an rRNA operon, one of the most highly transcribed operons. Replication fork progression, monitored by EM, was much slower when running against, rather than with, the direction of transcription. Plasmid DNA replication in *E. coli* can also be hindered by head-on transcription from a strong inducible promoter, probably because of collisions between the replisome and RNAP (ref. 11 and references therein). Head-on transcription of tRNA genes in eukaryotes can also cause pausing of replication (12).

These findings generally confirmed suggestions that coorienting transcription and replication of highly expressed genes might confer an evolutionary advantage by reducing obstruction of replication fork progression (6, 13). Consistent with this hypothesis, genes encoding rRNA coorient with replication in *E. coli*, most other bacteria, and eukaryotes (refs. 13–16 and references therein). Coorientation bias is also prominent for other highly transcribed genes (e.g., refs. 6, 7, 17, and 18).

Most genes are not as highly expressed as rRNA genes. Among the >4,000 genes in *E. coli*, the seven rRNA operons can constitute ≈50% of RNA synthesis. Yet, there is still a strong coorientation bias throughout the genomes of most bacteria, including *Bacillus subtilis*.

B. subtilis contains a single circular chromosome with one origin of replication (*oriC*) located at 0°/360° (Fig. 1*A*). Replication is bidirectional with clockwise (right) and counterclockwise (left) replication forks that meet in the terminus region (≈172°). There is a strong bias (75%) for codirectional transcription and replication in both arms (19), indicating that there is evolutionary pressure for coorientation throughout the genome (7). Also, essential genes are often encoded on the leading strand, independently of their expression (20, 21).

Except for a few highly transcribed *E. coli* genes, it is not known whether the genome-wide bias to coorient transcription and replication reduces replication problems. In addition, potential problems with transcription, including interruptions in gene expression and production of potentially toxic truncated polypeptides, could increase with head-on replication. It was suggested that these problems contribute to selective pressures to coorient transcription and replication (e.g., refs. 5, 7, and 21).

We investigated the effects of altering the coorientation bias of transcription and replication on replication fork progression in *B. subtilis* by using DNA microarrays. We compared rates of replication between wild-type and mutant strains in which the coorientation bias was altered (Fig. 1). Taking advantage of the strong bias in both chromosomal arms, the single origin of replication, and the ability to easily manipulate the genome, we constructed mutants with an origin of replication located away from 0° (Fig. 1). Each mutant has an extended region in which replication and most transcription are head-on rather than cooriented. We found that in wild-type cells (75% coorientation), replication proceeded without detectable interference from transcription. In contrast, replication elongation in the mutants was impeded in the regions with reversed bias. The reduction in replication was throughout the region and not limited to highly expressed rRNA operons or specific locations.

Author contributions: J.D.W. and A.D.G. designed research; J.D.W. and M.B.B. performed research; J.D.W. and M.B.B. contributed new reagents/analytic tools; J.D.W. and A.D.G. analyzed data; and J.D.W., M.B.B., and A.D.G. wrote the paper.

The authors declare no conflict of interest.

This article is a PNAS Direct Submission.

Abbreviation: RNAP, RNA polymerase.

*Present address: Department of Molecular and Human Genetics, Baylor College of Medicine, One Baylor Plaza, Room S-911, Houston, TX 77030.

†To whom correspondence should be addressed. E-mail: adg@mit.edu.

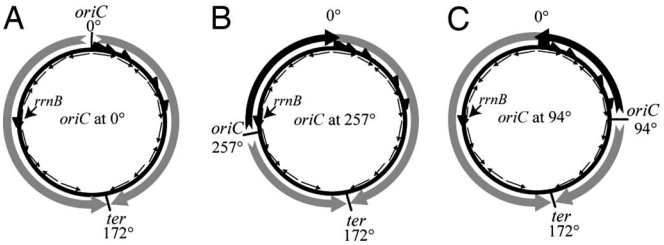

Fig. 1. Organization of replication and transcription in wild-type (*A*, *oriC* at 0°) and mutants (*B*, *oriC* at 257° and *C*, *oriC* at 94°). *oriC*, origin of replication; *ter*, terminus of replication; big gray arrows, replication in regions where the bulk of transcription is codirectional; big black arrows, replication in regions where the bulk of transcription is head-on; small arrows, symbolic representation of orientation of bulk transcription units; arrowheads, ribosomal RNA operons with the indicated directionality (only *rrnB* is labeled). There are 10 *rrn* operons: *rrnO* at 1°; *rrnA* at 3°; *rrnJ* and *rrnW* at 7–8°; *rrnH*, *rrnI*, and *rrnG* at 13–15°; *rrnE* at 54°; *rrnD* at 80°; and *rrnB* at 271°. For clarity, only some are indicated.

Inhibiting transcription brought the rate of replication back to normal, indicating that transcription was responsible for impeding replication. Our results demonstrate that replication is impeded by head-on transcription on a genome-wide scale and support the idea that a significant part of the selective pressure driving the bias to coorient transcription and replication comes from effects on replication.

Results

Transcription Does Not Detectably Affect Replication Elongation in Wild-Type Cells. We monitored DNA content and replication fork progression in synchronously replicating *B. subtilis* cells by using microarrays to measure the relative amount of DNA for almost all ORFs (22–24). We synchronized replication in a population of cells by using a mutant (*dnaB134*) that was temperature-sensitive for the initiation of replication, essentially as described (25, 26).

Twenty minutes after synchronous release of replication forks, gene dosage near *oriC* increased to approximately twice that of genes further away (Fig. 2*A*), indicating that replication initiation took place in almost all cells. The position of the forks is determined by the regions of the graph where the gene dosage rises higher than one ($\log_2 = 0$). The positions of the forks were approximately symmetric from *oriC*; both forks replicated up to ≈0.5 Mbp from *oriC*, as observed previously (22).

Forty minutes after initiation of replication, both forks had progressed up to ≈1.2 Mbp from *oriC* (Fig. 2*B*). In addition, gene dosage near *oriC* increased to ≈2.3-fold greater than that of genes not yet replicated because of replication reinitiation in a subpopulation of cells (26).

We examined the effect of inhibiting transcription on replication fork progression. Transcription was inhibited 20 min after initiation of replication by adding rifampicin, and samples were taken to measure DNA content 20 min later. The positions of the forks were similar in treated and untreated cells (Fig. 2 *C* and *D*). As expected, we did not observe replication reinitiation when transcription was inhibited (Fig. 2*C*). We conclude that transcription does not detectably affect replication elongation in strains with the wild-type coorientation bias.

There is some cell-to-cell variation in the distance that the forks progressed. If replication were absolutely synchronous in all cells, then there would be a sharp transition represented by a vertical line at the position of the forks. Instead, there was a slope between the front and back edges of the forks. This heterogeneity is probably due to variations in the timing of initiation and the rate of elongation.

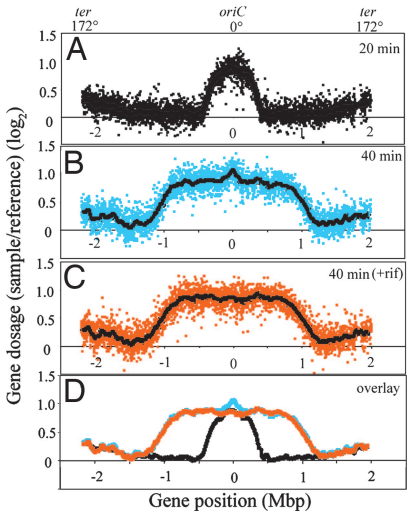

Fig. 2. Replication elongation was not affected by transcription in cells with the wild-type chromosomal organization. KPL151 (*oriC* at 0°; *dnaB134ts*) was grown in minimal glucose medium at 30°C, shifted to 45°C for 30 min, then back to 30°C to allow initiation of replication. Relative gene dosage was determined by cohybridization of replicating and preinitiation reference DNA to the microarrays, and plotting the ratio on the *y* axis ($\log_2$) against the corresponding gene positions on the *x* axis. 0°/360° is located in the middle; 172° (the terminus) is to both the left and the right. Each data point represents dosage of a single ORF. Lines are drawn for the rolling averages. (*A*) DNA profile 20 min after initiation of replication. (*B* and *C*) DNA profiles 40 min after initiation of replication without (*B*) or with (*C*) rifampicin (0.25 mg/ml; to inhibit transcription) added 20 min after initiation of replication. The slight increase in gene dosage near the terminus is probably due to incomplete replication in the preinitiation reference sample. (*D*) Overlay of the averaged genomic profiles from *A* to *C*. *A*, gray; *B*, blue; *C*, orange.

Replication Fork Progression Slows in a Region with Reversed Coorientation Bias. We analyzed replication fork progression in a mutant in which the orientations of replication and transcription are opposed over an extended segment of the chromosome (≈1.2 of ≈4.2 Mbp). We constructed this mutant by moving *oriC* from 0° to 257° while maintaining the organization of the rest of the chromosome (27) (Fig. 1*B*). This strain is viable but grows slowly, especially in rich medium (27). To reduce adverse effects, cells were grown in minimal medium with the relatively poor carbon source fumarate.

We compared the replication pattern of a strain with *oriC* at 0° (Fig. 3 *A–C*) to that of a mutant strain with *oriC* at 257° (Fig. 3 *D–F*). The replication cycle was synchronized, and 20 min after initiation, gene dosage near *oriC* increased by ≈60% when *oriC* was at 0° (Fig. 3*A*) and ≈40% when *oriC* was at 257° (Fig. 3*D*), indicating that DNA replication initiated in a subpopulation of cells.

In the strain with *oriC* at 0°, the left and right forks replicated approximately equal distances (Fig. 3*A*). In contrast, in the strain with *oriC* at 257°, the positions of the two replication forks were quite different (Fig. 3*D*). In cells with *oriC* at 257°, the slope between the front and the back edge of the replication forks is not as steep as that in cells with *oriC* at 0°, probably because replication initiation from 257° is less synchronous than that from 0°. Despite this asynchrony, the positions of the front edge of the forks can be identified, and there is an unambiguous asymmetry between the left and right forks initiating from *oriC* at 257°. The left (counterclockwise) fork replicated up to ≈0.64 Mbp from *oriC*, whereas the right (clockwise) fork, which replicates against the major direction of transcription, replicated only up to ≈0.42 Mbp during the same time period (Fig. 3*D*).

We calculated the average positions of the replication forks for

MICROBIOLOGY

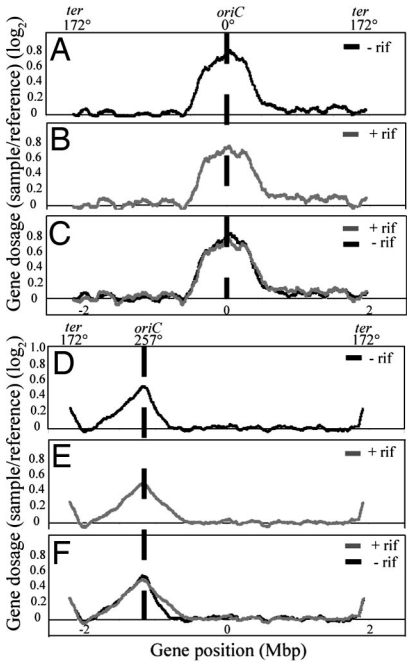

Fig. 3. Replication elongation is slowed by head-on transcription. Replication was monitored by DNA microarrays and the rolling average of data points was plotted as in Fig. 2. *dnaBts* strains KPL151 (*oriC* at 0°) (*A–C*) and JDW207 (*oriC* at 257°) (*D–F*) were grown in minimal fumarate medium at 30°C, shifted to 45°C for 60 min, then back to 30°C to allow initiation of replication. The efficiency of replication initiation was typically lower than that of cells grown in glucose (Fig. 2), perhaps due to the decreased growth rate in fumarate. We have not explored this difference. (*A* and *D*) Microarray profiles 20 min after initiation of replication. Vertical bars indicate the position of *oriC*. (*B* and *E*) Microarray profiles 20 min after initiation of replication, with rifampicin (0.25 mg/ml) added 4 min after temperature shift-down. (*C* and *F*) Overlay of microarray profiles without (black; −rif) and with (gray; +rif) rifampicin.

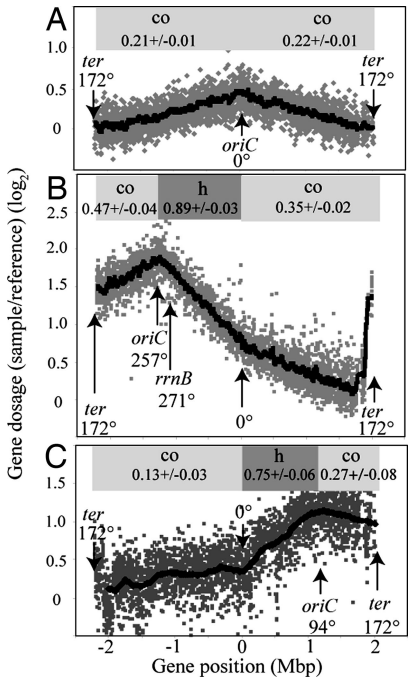

Fig. 4. DNA content in asynchronously growing cells. Cells were grown in minimal fumarate medium at 37°C (*A* and *B*) or 30°C (*C*). co, regions where replication and the bulk of transcription are cooriented; h, regions where replication and the bulk of transcription are head-on. The slopes of each segment of the plots are indicated (±2 × standard error). 0°, *oriC*, *ter*, and *rrnB* are indicated. The strain with *oriC* at 94° grows much more poorly than the others and there is much more scatter in the data. (*A*) Wild-type cells with *oriC* at 0° (JH642). (*B*) 257°::*oriC* Δ*oriC-L* (MMB703). (*C*) 94°::*oriC* Δ*oriC-L dnaB134ts* (JDW258).

the strain with *oriC* at 257°. We fit all of the microarray data points between *oriC* and the front of the replication forks to a linear equation. The average position of the forks in the codirectional region was 0.33 ± 0.02 Mbp from *oriC*, whereas that in the head-on region was 0.20 ± 0.01 Mbp from *oriC*. We conclude that replication fork progression slows in the region with reversed coorientation bias of transcription and replication.

The Decrease in Fork Progression in the Region with Reversed Coorientation Bias Depends on Transcription. We tested the effects of blocking transcription on replication fork progression during a synchronous replication cycle. We inhibited transcription by adding rifampicin 4 min after synchronous release of replication forks. The 4-min delay ensured that inhibiting transcription did not block initiation of replication on temperature shift-down. In the strain with *oriC* at 0°, adding rifampicin after replication initiation had no detectable effect on replication fork progression (Fig. 3 *B* and *C*).

In contrast, the replication profile of the strain initiating from 257° was altered by addition of rifampicin. The right fork replicated up to ≈0.62 Mbp from *oriC* in the presence of rifampicin (Fig. 3 *E* and *F*), compared with ≈0.42 Mbp in the absence of rifampicin (Fig. 3 *D* and *F*). The average position of the right fork changed to 0.33 ± 0.02 Mbp from 0.20 ± 0.01 Mbp, indicating that the rate of replication had increased in the presence of rifampicin. The left fork (codirectional region) was not significantly affected. It had replicated up to ≈0.64 Mbp from *oriC* in both conditions and the average position was 0.33 ± 0.02 Mbp in the absence and 0.31 ± 0.02 Mbp in the presence of rifampicin (Fig. 3 *D* and *F*). We conclude that the reduced replication rate in the region with reversed coorientation bias is a consequence of transcription. Furthermore, the decrease in replication elongation is not due to a trans-acting factor generally affecting replication because the decrease is limited to the region with reversed bias.

Replication Fork Progression Is Impeded Throughout the Region with Reversed Coorientation Bias. The decreased progression of replication forks in the region with head-on transcription and replication could be due to reduced replication throughout the region or head-on transcription at a specific locus. For example, the highly expressed *rrnB* operon at 271° is encountered by the right replication fork originating from 257° within 20 min after replication initiation. *rrnB* transcription is normally aligned with replication, but is against replication in strains with *oriC* at 257° (Fig. 1 *A* and *B*). In *E. coli*, replication of an rRNA operon in the head-on orientation takes >6 min compared with ≤6 sec when cooriented (10).

To distinguish between these two possibilities, we monitored the rate of replication elongation throughout the chromosome by measuring gene dosage in cells growing asynchronously (Fig. 4). For asynchronously growing cells, the slope of a plot of gene dosage ($\log_2$) as a function of its chromosomal position is proportional to the frequency of initiation and inversely proportional to the rate of elongation of replication. (This pattern differs from that for synchronous cells, whose slopes are inversely proportional to replication fork heterogeneity.) Even if there are different frequencies of initiation between strains, it is possible to compare the clockwise and counterclockwise forks in a given strain because each fork originates from a single bidirectional origin. If there is a specific locus that causes the

decreased fork progression, then there should be a discontinuity in the slope of such a plot at that locus. Our results (below) indicate that fork progression decreased throughout the head-on region and that there did not seem to be a sharp discontinuity within that region.

In wild-type cells growing asynchronously, gene dosage decreased with increasing distance from *oriC* at 0° (Fig. 4*A*) as expected. The slopes counterclockwise and clockwise from *oriC* were essentially the same (0.21 ± 0.01 and 0.22 ± 0.01, respectively), indicating that the rate of replication elongation is similar throughout the chromosome.

In mutant cells with *oriC* at 257° growing asynchronously, gene dosage decreased with increasing distance from 257° (Fig. 4*B*) as expected. Most noticeably, the slope clockwise from *oriC* (0.89 ± 0.03) in the head-on region (257°–360°) was steeper than that counterclockwise from *oriC* (0.47 ± 0.04) in the codirectional region (257°–172°). Because the two forks are generated from the same initiation event at *oriC*, the difference in slopes reflects a difference in the rate of replication and a steeper slope indicates that replication elongation is slower. The steeper slope was limited to the head-on region. Once the clockwise fork passed 0° and entered the codirectional region (0°–172°), the rate of replication increased. The slope changed at the 0° boundary from 0.89 ± 0.03 to 0.35 ± 0.02. This slope (0.35 ± 0.02) was still different from that observed in the codirectional region from 257° to 172°. We suspect that this difference is due to a subpopulation of the replication forks not making it all of the way through the head-on region and thus fewer forks entering the codirectional region from 0° to 172°.

The apparent linearity of the DNA profile throughout the head-on region indicates that replication is not slowed specifically in *rrnB* or another locus, but rather is slowed throughout the region.

We observed similar effects on replication elongation when *oriC* was moved from 0° to 94° (Figs. 1*C* and 4*C*). As expected, replication initiated from 94° and fork progression was slower in the region in which replication and most transcription were head-on. The slope (0.75 ± 0.06) counterclockwise from *oriC* in the head-on region was steeper than that clockwise from *oriC* in the codirectional region (0.27 ± 0.08). These results are consistent with those from the strain with *oriC* at 257°. For unknown reasons, strains with *oriC* at 94° are sicker than those with *oriC* at 257° and we were unable to achieve sufficient and reproducible synchrony with *oriC* at 94° to do experiments analogous to those in Fig. 3.

Inhibition of Replication Elongation in the Head-On Region Is Independent of *oriC*. During asynchronous growth, the strain with *oriC* at 257° (Fig. 4*B*) had a higher gene dosage, especially around *oriC*, than the strain with *oriC* at 0° (Fig. 4*A*). The slope (0.47 ± 0.04) in the codirectional region from 257° to 172° was steeper than that for cells with *oriC* at 0° (≈0.21 ± 0.01) (Fig. 4*A*). These differences indicate that replication initiation is more frequent in the strain with *oriC* at 257°. This is probably due to DnaA-dependent feedback regulation of replication initiation by replication elongation. Initiation at *oriC* can be stimulated when elongation is inhibited (23, 28). In the strain with *oriC* at 257°, replication of one arm of the chromosome takes much less time than replication of the other. In addition, head-on transcription and replication appear to cause induction of the SOS response (see *Discussion*), which can also cause an increase in DnaA-dependent replication initiation at *oriC* (23, 28). We postulate that a significant effect of having *oriC* at 257° is to cause an increase in DnaA-dependent replication initiation.

The increase in replication initiation in the strain with *oriC* at 257° was not observed during the synchronous initiation of replication (Fig. 3 *A* versus *D*). There was typically a lower efficiency of initiation in cells with *oriC* at 257°, perhaps due to slower growth of the mutant. Reduced efficiency is consistent with the notion that the increase in replication initiation in asynchronous cultures is due to feedback control by replication elongation. In the synchronous culture (*dnaBts*), replication is allowed to mostly finish at a temperature that prevents replication initiation. Thus, upon shift to permissive temperature and initiation of replication, the feedback controls will mostly have been eliminated for the first round of initiation.

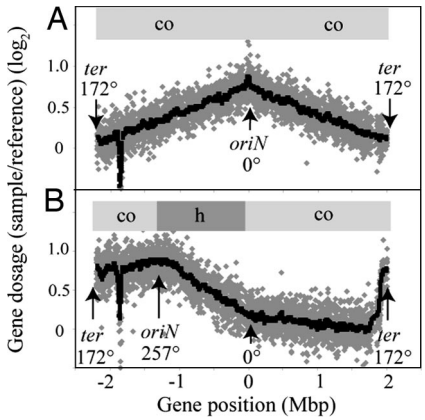

Fig. 5. DNA content in asynchronously growing cells whose replication initiates from *oriN*. Cells were grown in minimal fumarate medium at 37°C. Notations are as in Fig. 4. These strains have a deviation in sequence from approximately *ypjG* (201°) to approximately *hepT* (204°), causing a drop in the signals for most genes in this region relative to the reference strain JH642 (27). (*A*) 359°::*oriN* Δ*oriC-S* (MMB208). (*B*) 257°::*oriN* Δ*oriC-S* (MMB700).

The increase in replication initiation noted above required the DnaA-dependent *oriC*. We used strains (27) that have *oriC* inactivated and that initiate replication from the *dnaA*-independent heterologous origin *oriN* (29, 30). In asynchronous growth, the amount of replication initiation from *oriN* at 359° (Fig. 5*A*) was similar to that from *oriN* at 257° (Fig. 5*B*).

The cells initiating replication from *oriN* at 257° had a significant decrease in the rate of replication elongation in the region of head-on transcription and replication compared with the codirectional regions (Fig. 5*B*), consistent with the results in cells initiating from *oriC* at 257° (Fig. 4*B*). Therefore, the decrease in replication elongation is independent of the identity of the origin of replication.

Altered Relative Gene Dosage in the Terminus Region in Strains with Ectopic Origins. There was significant asymmetry in gene dosage near the terminus region (≈172°) in strains with origins away from 0°. In the wild-type strain, gene dosage at positions just >172° was similar to that at positions just <172° (Fig. 4*A*). In contrast, in the strains with *oriC* or *oriN* at 257°, gene dosage at positions just <172° was significantly less than that at positions just >172° (Figs. 4*B* and 5*B*). In the strain with *oriC* at 94°, gene dosage at positions >172° was significantly less than that at positions <172° (Fig. 4*C*). These differences in gene dosage are probably due to efficient replication arrest in the terminus region and the increased time it takes to replicate the longer arm of the chromosome in the mutants. This increased time is due to the combined effects of the increased distance and the slower rate of replication throughout the head-on region.

Discussion

In most bacteria, there is a genome-wide bias for genes to be encoded on the leading strand, resulting in coorientation of transcription and replication. We found that reversing this coorientation bias in *B. subtilis* impedes replication elongation and that this impediment depended on transcription. The decrease (≈40–50%) in the rate of replication elongation occurred only in the chromosomal region with the reversed bias, indicating that it is not due to trans-acting genome-wide events. Previous studies established that

MICROBIOLOGY

interference from head-on transcription of strongly expressed genes can reduce the rate of replication elongation in *E. coli* (e.g., see refs. 10 and 11). Our findings indicate that the reduction in the rate of replication occurs on a genomic scale in the region with reversed bias.

The reduction in replication due to head-on transcription could conceivably be due to a uniform decrease in the rate of DNA synthesis throughout the region. However, it seems more probable that the reduction in fork progression is due to frequent pauses and stops in the head-on region. Our results support the hypothesis that deleterious effects on replication caused by head-on transcription provide significant evolutionary pressure for developing the coorientation bias of transcription and replication in *B. subtilis*.

Strand Biases in *E. coli* and Phage. In contrast to *B. subtilis*, *E. coli* has a weak genome-wide coorientation bias (55%). It was suggested that this difference in coorientation bias might be due to different rates of replication between the two organisms (31), or the use of different types of DNA polymerases (32). *B. subtilis* and other bacterial species that use two types of replicative DNA polymerase (PolC and DnaE) typically have stronger coorientation bias than bacteria such as *E. coli* that use only DnaE. Despite the weak bias for coorientation overall in *E. coli*, there is a strong bias for coorientation of highly transcribed genes (e.g., see refs. 6, 7, and 13).

Effects of collisions between DNA and RNA polymerases have been studied *in vitro* for bacteriophages T4 and ϕ29, both of which encode their own replication machinery. The replication apparatus from T4 phage can bypass *E. coli* RNAP in head-on and codirectional orientations after pausing times of $\approx$1.7 sec and $<$1 sec, respectively (33, 34). DNA polymerase from ϕ29 can bypass *B. subtilis* RNAP during head-on encounters. During codirectional encounters, the ϕ29 DNA polymerase slows down and follows RNAP (35, 36).

These alternative strategies to reduce the conflict of transcription and replication might have arisen because the mechanisms used for initiating T4 and ϕ29 replication make it hard to select for strong coorientation bias. ϕ29 does not have a lagging strand; it initiates replication from each end of the double-stranded phage DNA (37). For its initial round of replication, T4 uses a site-specific origin of replication. T4 then uses recombination to initiate replication, essentially at random places throughout its genome (38).

Uncoupling of Replication Forks. The differences in progression of replication forks in the codirectional and head-on regions in the mutant strains (Fig. 3 *D–F*) indicate that the clockwise and counterclockwise forks are uncoupled. In addition, we observed a slight asymmetry in replication from *oriC* at 0° (ref. 27 and Fig. 3 *A–C*). There was typically a higher dosage of genes just to the right of *oriC* compared with the left, indicating that one replication fork was slightly ahead (10–50 kb) of the other (22). This difference was more obvious in cells grown in fumarate, where the frequency of initiation and synchrony are reduced relative to that in cells grown in glucose (compare Figs. 2 and 3). The asymmetry between the two forks is similar to results with *E. coli* (24) and indicates that the two forks need not be coupled.

Selective Pressures for Coorientation of Transcription and Replication. Based on the observations that essential and highly expressed genes possess stronger bias to be encoded in the leading strand (refs. 5, 7, and 21 and references therein), several processes have been proposed to contribute to the selective pressures for the coorientation of transcription and replication. We suspect that the most significant effects are due to selective pressure for efficient replication (below). In addition to effects on replication, collisions between RNA and DNA polymerases are expected to cause a small decrease in transcription of a given gene when the replication fork passes through. This decrease should be somewhat larger for head-on collisions than for codirectional collisions (5, 7). Such decreases are expected to be too small to be reliably measured, but might cause decreased fitness (7). Head-on collisions are also speculated to cause production of truncated mRNA and potentially toxic truncated polypeptides (20, 21). There are mechanisms for eradicating such products (39), but there might be a decrease in fitness with increased production of truncated products.

Whereas these processes may contribute to selection for the coorientation of transcription and replication, it seems probable that the major contribution is from problems with replication. There are at least two significant deleterious effects on replication due to head-on transcription. First, the reduced rate of replication in the chromosomal region with reversed coorientation bias would increase the amount of time needed for genomic duplication and probably limit cell cycle progression. Second, head-on collisions can lead to replication fork arrest, potentially causing the generation of deletions and other mutations, and possibly inducing the SOS response.

In preliminary experiments, we noticed that the strain with *oriC* at 257° has increased expression of some SOS (damage-inducible) genes. Expression of these genes is known to be induced when replication is disrupted (23, 28), and we suspect that obstruction of replication elongation within the head-on region may cause some induction of the SOS response. Pile-up of replication forks in the terminus region because of unbalanced replicores might induce replication fork collapse as suggested for *E. coli* (40) and perhaps contribute to induction of the SOS response. If SOS induction is due, even in part, to head-on collisions between RNA and DNA polymerases, then this could cause decreased fitness.

Disruption of replication forks can result in failure to complete replication, or cause recombination and mutagenesis at the stalled forks during attempts to restart replication (41). In asynchronous cultures of mutants with significant head-on regions, the slopes (gene dosage vs. position) were different in the two codirectional regions (Figs. 4 *B* and *C* and 5*B*), indicating that some replication forks in the head-on region fail to complete replication. Blocks to replication can stimulate illegitimate recombination and deletions in *E. coli* (42). Paused replication forks can lead to double-strand breaks (41, 43, 44) and there is evidence of increased mutagenesis in the local region of double-strand breaks (45). Essential genes are greatly enriched among transcripts cooriented with replication (20, 21), probably because cells are more sensitive to mutations in essential genes and it is important to avoid disruption of their replication by head-on transcription (11). Highly expressed genes are also enriched among the cooriented transcripts (7), probably because transcription from these genes would disrupt replication more frequently when oriented opposite to replication. The coorientation arrangement of transcription and replication in bacterial genomes might be an effective means for cells to increase the efficiency of replication and reduce the occurrence of genomic instability.

Materials and Methods

Strains. Standard procedures were used for genetic manipulations and strain constructions (46). Strains used and relevant genotypes include JH642 (*trpC2 pheA1*); KPL151 [*trpC2 pheA1 dnaB134ts-zhb83*::Tn*917*(*cat*)]; JDW207 [*trpC2 pheA1 argG*(257°)::(*oriC*/*dnaAN kan*) Δ(*oriC-L*)::*spc dnaB134ts-zhb83*::Tn*917*(*cat*)]; JDW258 [*trpC2 pheA1 aprE*(94°)::(*oriC*/*dnaAN kan*) Δ(*oriC-L*)::*spc dnaB134ts-zhb83*::Tn*917*(*cat*)]; MMB703 [*trpC2 pheA1 argG*(257°)::(*oriC*/*dnaAN kan*) Δ(*oriC-L*)::*spc* (27)]; MMB208 [*pheA1* (*ypjG-hepT*)*122 spoIIIJ*(359°)::(*oriN kan tet*) Δ*oriC-S*]; and MMB700 [*pheA1* (*ypjG-hepT*)*122 argG*(257°)::(*oriN kan*) Δ*oriC-S*].

MMB208, MMB700, and MMB703 were constructed as described in ref. 27, by integrating an origin (*oriC* or *oriN*) at an ectopic site and then inactivating *oriC* at 0°.

JDW207 was constructed by transforming chromosomal DNA

from KPL151 (*dnaBts cat*) into MMB703, selecting for *cat*, and testing for *dnaBts*.

JDW258 was constructed by integrating a second *oriC* into *aprE*(94°) in KPL151 to obtain JDW231, then deleting *oriC* at 0° by transforming chromosomal DNA from MMB703 and selecting for *spc*.

To obtain JDW231, *kan*, flanked by *aprE* front and back segments, was subcloned into pBR322 digested with EcoRI/SphI to produce the 94° integration plasmid pMMB724. Plasmid pJDW113 was constructed by subcloning *oriC* from pMMB574 (27) digested with KpnI/BamHI into pMMB724. Linearized pJDW113 was transformed into KPL151 selecting for *kan*.

Δ(*oriC-L*)::*spc* replaces all of the *dnaAN* operon (inactivating *oriC*) with *spc*, as described in refs. 27 and 28. Δ*oriC-S* is a deletion of 152 bp downstream of *dnaA* and inactivates *oriC*. It is almost identical to *oriC-6* (30).

oriN is derived from a low-copy *Bacillus* plasmid and requires RepN for initiation of replication. When integrated into the chromosome, it supports *dnaA*-independent bidirectional replication in slowly growing cells (29, 30).

Media and Growth Conditions. Cells were grown in LB or in S7 minimal medium (50 mM Mops), with 1% glucose or sodium fumarate, 0.1% glutamate, and supplemented with 40 μg/ml tryptophan, 40 μg/ml phenylalanine, or 400 μg/ml arginine, as needed.

Replication was synchronized as described in refs. 22, 25, and 26. Briefly, *dnaB134ts* strains were incubated at 45°C for 30 min in minimal glucose medium, or 60 min in minimal fumarate medium, to prevent new rounds of replication from initiating and to allow most ongoing rounds to finish. Cultures were then shifted to 30°C by rapidly mixing them with 1.5 vol of fresh medium at 20°C to allow new rounds of replication to start.

Microarrays and Data Analysis. Microarrays contained PCR products from >99% of the annotated *B. subtilis* ORFs (22, 23, 28). Cells were collected and mixed with an equal volume of ice-cold methanol. Relative amounts of DNA for each ORF are plotted versus gene position. Data presented are from single representative experiments. Each experiment was done at least twice.

Data analysis was basically as described in ref. 24 except that programs in the MATLAB Curve Fitting Toolbox (Mathworks, Natick, MA) were used. Briefly, microarrays were scanned with a Genepix 4000B scanner (Axon Instruments, Union City, CA), and 16-bit TIFF images were acquired and analyzed with GenePix Pro (ver. 3.0.6.90). Spots were filtered to require that (*i*) diameters were >40 pixels; (*ii*) the signal was >3-fold above the local background determined for each spot; and (*iii*) after background subtraction, fluorescence was >200 intensity units in both channels and >1,000 intensity units in at least one channel. Typically, 75–95% of the spots satisfied these requirements, depending on the specific batch of arrays.

For synchronous replication, the region with the lowest relative abundance of DNA in the test sample was defined as "one." For asynchronous replication, the relative abundance from the terminus region was defined as "one."

Smoothed data were obtained by determining the rolling average of multiple contiguous data points and plotting the average to the middle position of these data points.

Slopes and average replication fork positions for the microarray replication profiles were determined from the primary data set (not the smoothed lines) by linear least square fitting to all data within each indicated region. The number of data pairs (gene position vs. relative gene dosage, $\log_2$) used for each ranged from ≈300 data points (Fig. 3*D*, the shortest region evaluated) to ≈2,000 data points (e.g., Figs. 4*A* and 5*A*, the longest regions spanning approximately half the chromosome). The 95% confidence intervals (which are indicated as $\pm 2 \times$ standard error) of the coefficients of the fit for each region are presented.

We thank J. Auchtung, A. Breier, A. Goranov, C. Lee, and L. Simmons for discussions and comments on the manuscript. J.D.W. was supported, in part, by the Damon Runyon Cancer Research Foundation (DRG-1768-03). M.B.B. was supported, in part, by a Jane Coffin Child postdoctoral fellowship. This work was supported by U.S. Public Health Service Grant GM41934 (to A.D.G.).

1. Hill CW, Gray JA (1988) *Genetics* 119:771–778.
2. Rebollo JE, Francois V, Louarn JM (1988) *Proc Natl Acad Sci USA* 85:9391–9395.
3. Campo N, Dias MJ, Daveran-Mingot ML, Ritzenthaler P, Le Bourgeois P (2004) *Mol Microbiol* 51:511–522.
4. Wu LJ, Errington J (2002) *EMBO J* 21:4001–4011.
5. Rocha EP (2004) *Microbiology* 150:1609–1627.
6. Brewer BJ (1988) *Cell* 53:679–686.
7. Price MN, Alm EJ, Arkin AP (2005) *Nucleic Acids Res* 33:3224–3234.
8. Mirkin EV, Castro Roa D, Nudler E, Mirkin SM (2006) *Proc Natl Acad Sci USA* 103:7276–7281.
9. Trautinger BW, Jaktaji RP, Rusakova E, Lloyd RG (2005) *Mol Cell* 19:247–258.
10. French S (1992) *Science* 258:1362–1365.
11. Mirkin EV, Mirkin SM (2005) *Mol Cell Biol* 25:888–895.
12. Deshpande AM, Newlon CS (1996) *Science* 272:1030–1033.
13. Nomura M, Morgan EA, Jaskunas SR (1977) *Annu Rev Genet* 11:297–347.
14. Guy L, Roten CA (2004) *Gene* 340:45–52.
15. Brewer BJ, Fangman WL (1988) *Cell* 55:637–643.
16. Rothstein R, Michel B, Gangloff S (2000) *Genes Dev* 14:1–10.
17. Zeigler DR, Dean DH (1990) *Genetics* 125:703–708.
18. McLean MJ, Wolfe KH, Devine KM (1998) *J Mol Evol* 47:691–696.
19. Kunst F, Ogasawara N, Moszer I, Albertini AM, Alloni G, Azevedo V, Bertero MG, Bessieres P, Bolotin A, Borchert S, *et al.* (1997) *Nature* 390:249–256.
20. Rocha EP, Danchin A (2003) *Nucleic Acids Res* 31:6570–6577.
21. Rocha EP, Danchin A (2003) *Nat Genet* 34:377–378.
22. Wang JD, Sanders GM, Grossman AD (2007) *Cell* 128, in press.
23. Goranov AI, Kuester-Schoeck E, Wang JD, Grossman AD (2006) *J Bacteriol* 188:5595–5605.
24. Breier AM, Weier HU, Cozzarelli NR (2005) *Proc Natl Acad Sci USA* 102:3942–3947.
25. Lemon KP, Grossman AD (2000) *Mol Cell* 6:1321–1330.
26. Henckes G, Harper F, Levine A, Vannier F, Seror SJ (1989) *Proc Natl Acad Sci USA* 86:8660–8664.
27. Berkmen MB, Grossman AD (2007) *Mol Microbiol* 63:150–165.
28. Goranov AI, Katz L, Breier AM, Burge CB, Grossman AD (2005) *Proc Natl Acad Sci USA* 102:12932–12937.
29. Hassan AK, Moriya S, Ogura M, Tanaka T, Kawamura F, Ogasawara N (1997) *J Bacteriol* 179:2494–2502.
30. Kadoya R, Hassan AK, Kasahara Y, Ogasawara N, Moriya S (2002) *Mol Microbiol* 45:73–87.
31. Omont N, Kepes F (2004) *Bioinformatics* 20:2719–2725.
32. Rocha E (2002) *Trends Microbiol* 10:393–395.
33. Liu B, Wong ML, Tinker RL, Geiduschek EP, Alberts BM (1993) *Nature* 366:33–39.
34. Liu B, Alberts BM (1995) *Science* 267:1131–1137.
35. Elias-Arnanz M, Salas M (1997) *EMBO J* 16:5775–5783.
36. Elias-Arnanz M, Salas M (1999) *EMBO J* 18:5675–5682.
37. Meijer WJ, Horcajadas JA, Salas M (2001) *Microbiol Mol Biol Rev* 65:261–287.
38. Miller ES, Kutter E, Mosig G, Arisaka F, Kunisawa T, Ruger W (2003) *Microbiol Mol Biol Rev* 67:86–156.
39. Withey JH, Friedman DI (2003) *Annu Rev Microbiol* 57:101–123.
40. Bidnenko V, Ehrlich SD, Michel B (2002) *EMBO J* 21:3898–3907.
41. Cox MM, Goodman MF, Kreuzer KN, Sherratt DJ, Sandler SJ, Marians KJ (2000) *Nature* 404:37–41.
42. Bierne H, Michel B (1994) *Mol Microbiol* 13:17–23.
43. Seigneur M, Bidnenko V, Ehrlich SD, Michel B (1998) *Cell* 95:419–430.
44. Kuzminov A (1995) *BioEssays* 17:733–741.
45. Ponder RG, Fonville NC, Rosenberg SM (2005) *Mol Cell* 19:791–804.
46. Harwood CR, Cutting SM (1990) *Molecular Biological Methods for Bacillus* (Wiley, Chichester, UK).